Supernova 2011fe from an exploding carbon-oxygen white dwarf star

Peter E. Nugent[1,2], Mark Sullivan[3], S. Bradley Cenko[2], Rollin C. Thomas[1], Daniel Kasen[1,4], D. Andrew Howell[5,6], David Bersier[7], Joshua S. Bloom[2], S. R. Kulkarni[8], Michael T. Kandrashoff[2], Alexei V. Filippenko[2], Jeffrey M. Silverman[2], Geoffrey W. Marcy[2], Andrew W. Howard[2], Howard T. Isaacson[2], Kate Maguire[3], Nao Suzuki[1], James E. Tarlton[3], Yen-Chen Pan[3], Lars Bildsten[6,9], Benjamin J. Fulton[5,6], Jerod T. Parrent[5,10], David Sand[5,6], Philipp Podsiadlowski[3], Federica B. Bianco[5,6], Benjamin Dilday[5,6], Melissa L. Graham[5,6], Joe Lyman[7], Phil James[7], Mansi M. Kasliwal[8], Nicholas M. Law[11], Robert M. Quimby[12], Isobel M. Hook[3,13], Emma S. Walker[14], Paolo Mazzali[15,16], Elena Pian[15,16], Eran O. Ofek[8,17], Avishay Gal-Yam[17] and Dovi Poznanski[1,2,18]

[1] *Lawrence Berkeley National Laboratory, Berkeley, CA, 94720, USA.*

[2] *Department of Astronomy, University of California, Berkeley, CA, 94720-3411, USA.*

[3] *Department of Physics (Astrophysics), University of Oxford, Keble Road, Oxford, OX1 3RH, UK.*

[4] *Department of Physics, University of California, Berkeley, CA, 94720, USA.*

[5] *Las Cumbres Observatory Global Telescope Network, Goleta, CA, 93117, USA.*

[6] *Department of Physics, University of California, Santa Barbara, CA, 93106, USA.*

[7] *Astrophysics Research Institute, Liverpool John Moores University, Birkenhead, UK.*

[8] *Cahill Center for Astrophysics, California Institute of Technology, Pasadena, CA, 91125, USA.*

[9] *Kavli Institute for Theoretical Physics, University of California, Santa Barbara, CA, 93106, USA.*

[10] *Department of Physics and Astronomy, Dartmouth College, Hanover, NH, USA.*

[11] *Dunlap Institute for Astronomy and Astrophysics, University of Toronto, 50 St. George Street, Toronto M5S 3H4, Ontario, Canada.*

[12] *IPMU, University of Tokyo, Kashiwanoha 5-1-5, Kashiwa-shi, Chiba, Japan*

[13] *INAF, Osservatorio Astronomico di Roma, via Frascati 33, 00040 Monteporzio (RM), Italy*

[14] *Scuola Normale Superiore, Piazza dei Cavalieri 7, 56126 Pisa, Italy*

[15] *INAF-Osservatorio Astronomico di Padova, vicolo dell'Osservatorio, 5 35122 Padova, Italy*

[16] *Max-Planck Institut fuer Astrophysik Karl-Schwarzschildstr. 1 85748 Garching, Germany*

[17] *Benoziyo Center for Astrophysics, The Weizmann Institute of Science, Rehovot 76100, Israel*

[18] *School of Physics and Astronomy, Tel-Aviv University, Tel-Aviv 69978, Israel*

1

Type Ia supernovae (SNe Ia) have been used empirically as standardized candles to reveal the accelerating universe[1–3] even though fundamental details, such as the nature of the progenitor system and how the star explodes, remained a mystery[4–6]. There is consensus that a white dwarf star explodes after accreting matter in a binary system, but the secondary could be anything from a main sequence star to a red giant, or even another white dwarf. The uncertainty stems from the fact that no recent SN Ia has been discovered close enough to detect the stars before explosion. Here we report early observations of SN 2011fe (PTF11kly) in M101 at a distance of 6.4 Mpc[7], the closest SN Ia in the past 25 years. We find that the exploding star was likely a carbon-oxygen white dwarf, and from the lack of an early shock we conclude that the companion was most likely a main sequence star. Early spectroscopy shows high-velocity oxygen that varies on a time scale of hours and extensive mixing of newly synthesized intermediate mass elements in the outermost layers of the supernova. A companion paper[8] uses pre-explosion images to rule out luminous red giants and most helium stars as companions.

SN 2011fe was detected on 2011 August 24.167 (UT 03:59) with a *g*-band magnitude of 17.35 by the Palomar Transient Factory (PTF) in the Pinwheel galaxy — Messier 101 (M101; see Figure 1). Observations on the previous night revealed no source to a limiting magnitude of 21.5. Given the distance to M101 of 6.4 Mpc[7], this first observation identified the supernova at an absolute magnitude of -11.7, roughly 1/1000 of its peak brightness.

Following an alert sent to the PTF consortium (at UT 19:51), observations were immediately undertaken by the *Swift* Observatory, and spectroscopic observations were carried out at UT 20:42 on the robotic Liverpool Telescope equipped with the FRODOSpec spectrograph (located at La Palma, Canary Islands). After the calibration of this spectrum, at UT 23:47 an Astronomer's Telegram was issued[9] identifying SN 2011fe as a young supernova of Type Ia. Eight hours later, a low-resolution spectrum was obtained with the Kast spectrograph at the Lick 3-m Shane telescope (Mt. Hamilton, California) and a high-resolution spectrum with HIRES at the Keck I telescope (Mauna Kea, Hawaii). These spectra are presented in Figure 2 (see Supplementary Information for details).

The discovery and extensive follow-up photometry allow us to estimate the time of explosion to high precision (Figure 3). At very early times the luminosity should scale as the surface area of the expanding fireball, thus is expected to rise as t^2, where t is the time since explosion. This assumes neither the photospheric temperature nor the velocity change significantly and the input energy from the radioactive decay of ^{56}Ni to ^{56}Co is relatively constant over this period and is near the photosphere. *Swift* observations show only small changes in the relative flux between the optical and ultraviolet, and the velocity evolution over the first 24 hr is small — consistent with these assumptions (see Supplementary Information).

Using the t^2 model, we find an explosion time at modified Julian date (MJD) 55796.696 ± 0.003 (see Figure 3). Letting the exponent of the power law depart from 2, which captures some of

the deviations from the fireball model, and fitting just the first 3 nights of data, results in a best-fit explosion date of 55796.687 ± 0.014 (UT 2011 August 23, $16:29 \pm 20$ minutes). The exponent of the power law is 2.01 ± 0.01, consistent with the model discussed above. Based on these fits, our first data points were obtained just over 11 hr after SN 2011fe exploded.

We analysed the Lick spectrum of SN 2011fe using the automated SN spectrum interpretation code SYNAPPS[10] (see Supplementary Information for further details). At this time only a few hundredths of a solar mass of material are visible above the photosphere, yet typical[11] pre-maximum SN Ia ions are seen: O I, Mg II, Si II, S II, Ca II, and Fe II are present at velocities of $16,000 \ \mathrm{km \, s^{-1}}$. The fit also shows the presence of C II $\lambda\lambda 6580, 7234$. Fe III was not needed in the fit. Both high-velocity (HV) Si II and Ca II are confirmed by SYNAPPS (extending above $21,000 \ \mathrm{km \, s^{-1}}$). Surprisingly, SYNAPPS finds HV O I (in excess of $20,000 \ \mathrm{km \, s^{-1}}$) for the absorption centered at 7400 Å. This feature has evolved significantly in only 8 hr, between the data taken at the Liverpool Telescope and Lick, with the absorption minimum receding from 18,000 to $14,000 \ \mathrm{km \, s^{-1}}$. The rapid evolution in these optically thin layers is best explained by geometrical dilution during the early phases. To our knowledge, this is the first identification of rapidly evolving high-velocity oxygen in the ejecta of a SN Ia.

The early-time spectra provide fundamental insight into the explosion physics of this SN. As in previous[12] SNe Ia, intermediate-mass elements dominate the spectrum. In addition, we see strong features from unburnt material (carbon and high-velocity oxygen). The overlap in velocity space implies that the explosion processed the outer layers of the progenitor white dwarf, but left behind (at least some) carbon and oxygen. The unburnt material could be confined to pockets, or the ejecta in the outer layers may be thoroughly mixed. The doubly ionised species (e.g., Si III and Fe III), often seen in the spectra of many early and maximum-light SNe Ia[13,14], are absent even though our observations are at ~ 1 day after explosion when the energy input from radioactive decay is near its peak. SN 2011fe is spectroscopically most similar to the slightly underluminous SNe Ia 1992A and 1994D[15,16], the latter of which also shows high-velocity features in the -12 day spectrum[17]. One potential explanation for this is that while some $^{56}\mathrm{Ni}$ has been mixed out to the photosphere, the majority produced in the explosion is confined to the innermost layers of the atmosphere, and thus the bulk of the heating is well separated from the portion of the atmosphere we view in these spectra.

The early detection of SN 2011fe allows us to put considerable constraints on the progenitor system of this SN Ia. At early times (about a day or less after explosion), radiative diffusion from the shock-heated outer layers of the ejecta is a contributor to the supernova luminosity. The origin of the shock can either be from a detonation of the WD[18] or a later collision with the companion star[19]. Dimensionally, the shock luminosity in this cooling, expanding envelope phase is $L \propto E(t)/t_d$, where $E(t)$ is the ejecta internal energy at the elapsed time t and t_d is the effective diffusion time through the homologously expanding remnant. Since the ejecta in these phases are heavily radiation dominated, the internal energy declines during adiabatic expansion as $E(t) \propto R_0/vt$, where R_0 is the initial radius of the star. Thus, the early-time luminosity is

proportional to R_0, while the effective temperature $T_{\text{eff}} \propto L^{1/4} \propto R_0^{1/4}$ (see also Supplementary Information).

While there must be radioactive heating in the outer layers of the SN, we can make the very conservative upper-limit approximation that the earliest g-band photometric point ($L \approx 10^{40}$ erg s^{-1} at ~ 0.5 day) is *entirely* due to the explosion. We then infer an upper limit to the radius of the progenitor star, $R_0 < 0.1\,R_\odot$ (Figure 4). This provides compelling, direct evidence that the progenitor of SN 2011fe was a compact star, namely a white dwarf. When we add the early carbon and oxygen observations, we conclude that the progenitor must have been a carbon-oxygen white dwarf.

The early-time light curve also constrains the properties of a binary star system[19], as the collision of the SN with a companion star will shock and reheat a portion of the ejecta. The resulting luminosity is proportional to the separation distance, a, between the stars, and will be most prominent for observers aligned with the symmetry axis. A red-giant companion predicts an early luminosity several orders of magnitude greater than that observed, and can be ruled out regardless of the viewing angle. A main-sequence companion is compatible with the data, unless SN 2011fe happened to be seen on-axis (within $\sim 40°$ of the symmetry axis), in which case the luminosity at day 0.5 rules out any binary with $a \leq 0.1\,R_\odot$.

Recent simulations of double-degenerate mergers have found that some material from the disrupted secondary WD may get pushed out to large radius (10^{13}–10^{14} cm), either in the dynamics of the merger[20] or in the subsequent long-term thermal evolution of the system[21]. The interaction of the ejecta with this roughly spherical medium should produce (for all viewing angles) bright, early UV/optical emission, in conflict with what is observed. Our restriction that the dense circumstellar medium must reside at $\leq 10^{10}$ cm thus presents a tight constraint for merger models, and only a few of those proposed thus far may be allowable for this SN[6].

Using some of the earliest photometry and spectroscopy ever obtained for a SN Ia, we have put more stringent limits than ever before achieved for a SN Ia on the progenitor of SN 2011fe, revealing that the primary is a carbon-oxygen white dwarf and the secondary is most consistent with being a main sequence star. We caution that these constraints rely on theoretical interpretation. A companion letter[8] uses independent methodology to place direct observational limits on the companion star from historical imaging ~ 100 times deeper than previous attempts.

These results are from only the first $\sim$ week of observation of SN 2011fe. This first close SN Ia in the era of modern instrumentation will undoubtedly become the best-studied thermonuclear supernova in history allowing daily study from the UV to the IR well into the faint nebular phase. As such, it will form the new foundation upon which our knowledge of more distant Type Ia supernovae is built.

Acknowledgments:

Author Contributions:

PEN, MS, and DAH oversee the PTF SN Ia program. PEN oversaw the preparation of the manuscript. MS, DB, KM, YCP, JL, and PJ executed and reduced the FRODOSpec observations. SBC, MTK, AVF, and JMS executed and reduced the Lick spectrum. GWM, AWH, and HTI obtained the HIRES observations. SBC, JSB, SRK, MMK, NML, EOO, RMQ, and DP assisted in the operation of P48 as part of the PTF collaboration. RCT and JET performed the SYNAPPS analysis. DK, LB, and PP assisted with the theoretical interpretation of our observations. NS, BJF, JTP, DS, FB, BD, MLG, IMH, PM, EP, EW, AG assisted in follow-up observations of SN 2011fe.

Correspondence and requests for materials should be addressed to Peter Nugent (e-mail: penugent@lbl.gov).
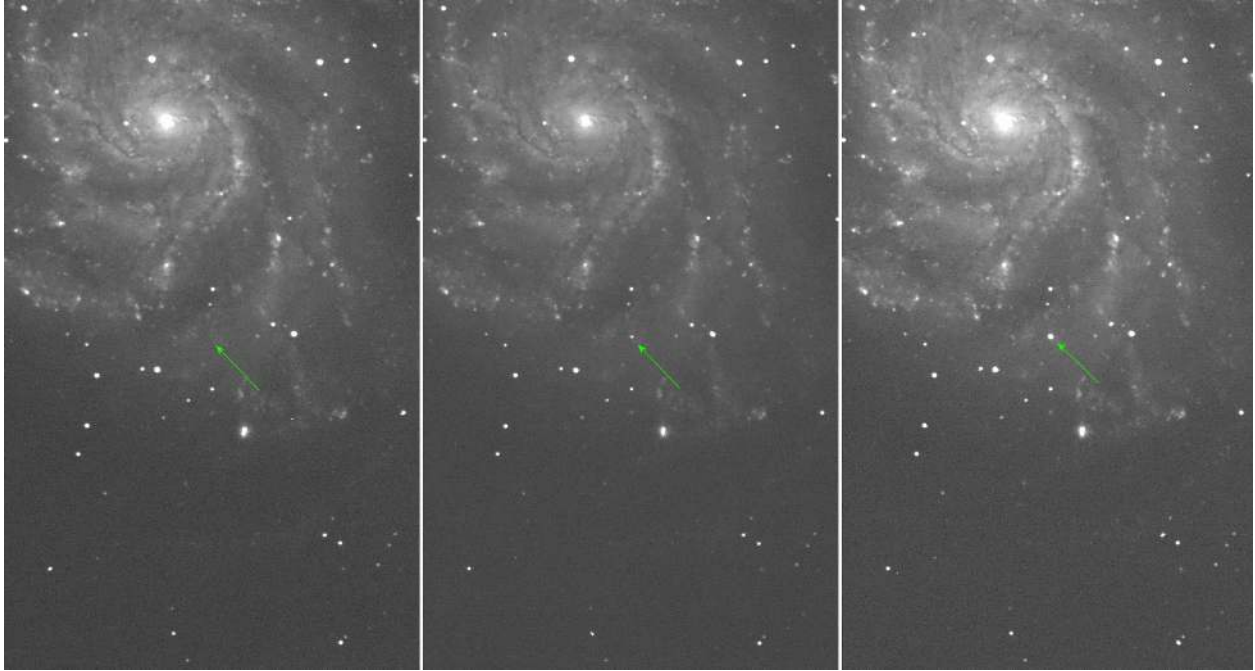
Figure 1: PTF *g*-band image sequence of the field of Messier 101 showing the appearance of SN 2011fe. From left to right, images are from August 23.22, 24.17, and 25.16 UT. The supernova was not detected on the first night to a 3-σ limiting magnitude of 21.5, was discovered at magnitude 17.35, and increased by a factor of 10 in brightness to mag 14.86 the following night. The supernova peaked at magnitude $\sim$9.9, making it the fifth brightest supernova in the past century. PTF is a wide-field optical experiment designed to systematically explore the variable sky on a variety of time scales, with one particular focus the very early detection of SNe[22, 23]. Discoveries such as this one have been made possible by coupling real-time computational tools to extensive astronomical follow-up observations[24, 25].
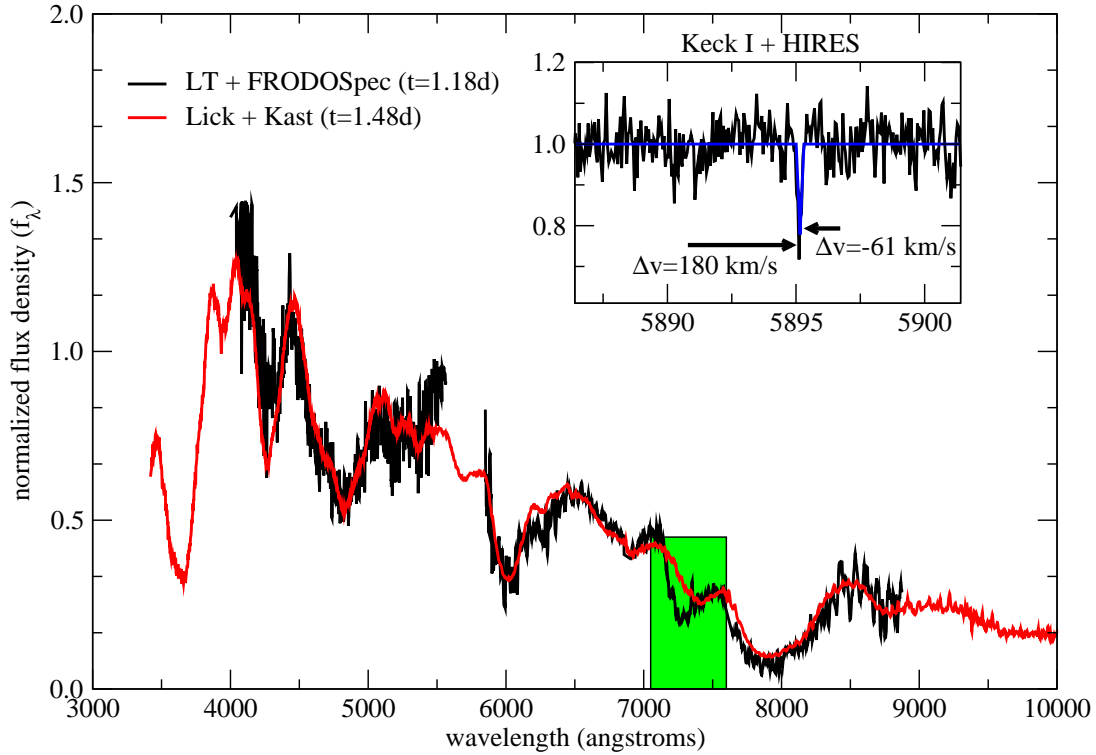
Figure 2: Spectra of SN 2011fe taken 1.5 days after explosion. Typical pre-maximum SN Ia ions are seen: O I, Mg II, Si II, S II, Ca II, and Fe II are present at photospheric velocities of 16,000 km s^{-1}. In addition, the fit shows the presence of C II $\lambda\lambda 6580, 7234$. Both high-velocity (HV) Si II and Ca II are seen (extending above 21,000 km s^{-1}), as is HV O I, the first evidence of such a feature in a SN Ia (green highlighted region). Note that this feature evolves in ~ 8 hr between the first two low-resolution spectra. *Inset:* A Keck+HIRES spectrum centered on the Na I D line. In this wavelength range, we identify only a single significant absorption feature. Fitting a Gaussian profile to it, we measure a central wavelength of $\lambda = 5893.75 \pm 0.02$ Å and a full width at half-maximum intensity (FWHM) of 0.184 ± 0.009 Å. The inferred line equivalent width is $W = 0.045 \pm 0.009$ Å. If we associate this feature with Na I $\lambda 5890$ (the stronger of the two components in the doublet), the observed wavelength is offset from the rest wavelength by $\Delta v = 194$ km s^{-1}. Similarly, the line is blueshifted from the systemic velocity of M101 ($v = 241 \pm 2$ km s^{-1};[26]) by $\Delta v_{M101} = -47$ km s^{-1}. Given the high Galactic latitude ($b = 59.8°$), we consider it likely that the absorbing material originates in M101 and the total extinction to the SN is negligible.
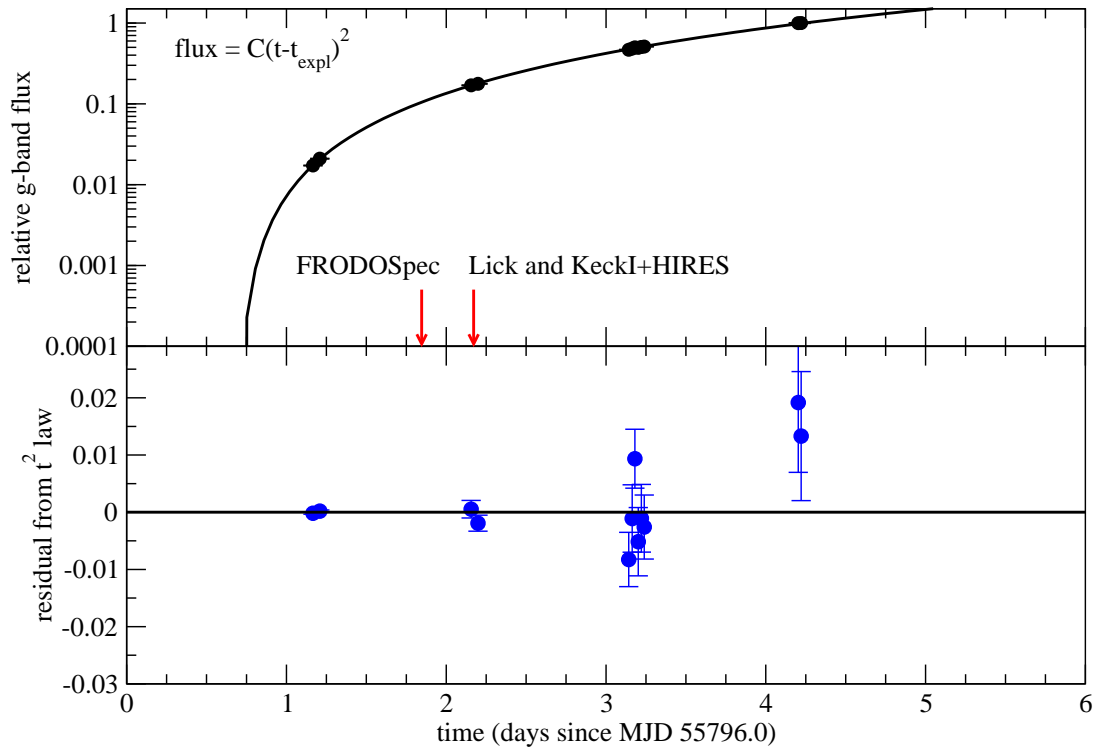
Figure 3: Early photometry of SN 2011fe shows a parabolic rise and constrains the time of explosion. *Top* The relative *g*-band flux as a function of time for the first 4 nights after detection. Here we have fit the rise with a t^2 fireball model. *Bottom* The residuals from the fit. Letting the exponent vary from 2, allowing for a potential departure from the fireball model, and only fitting the first 3 nights of data, we find a best-fit explosion date of August 23.687 ± 0.014 UT. Based on these fits, our first data points were obtained just over 11 hr after SN 2011fe exploded. All error bars presented are one standard deviation.
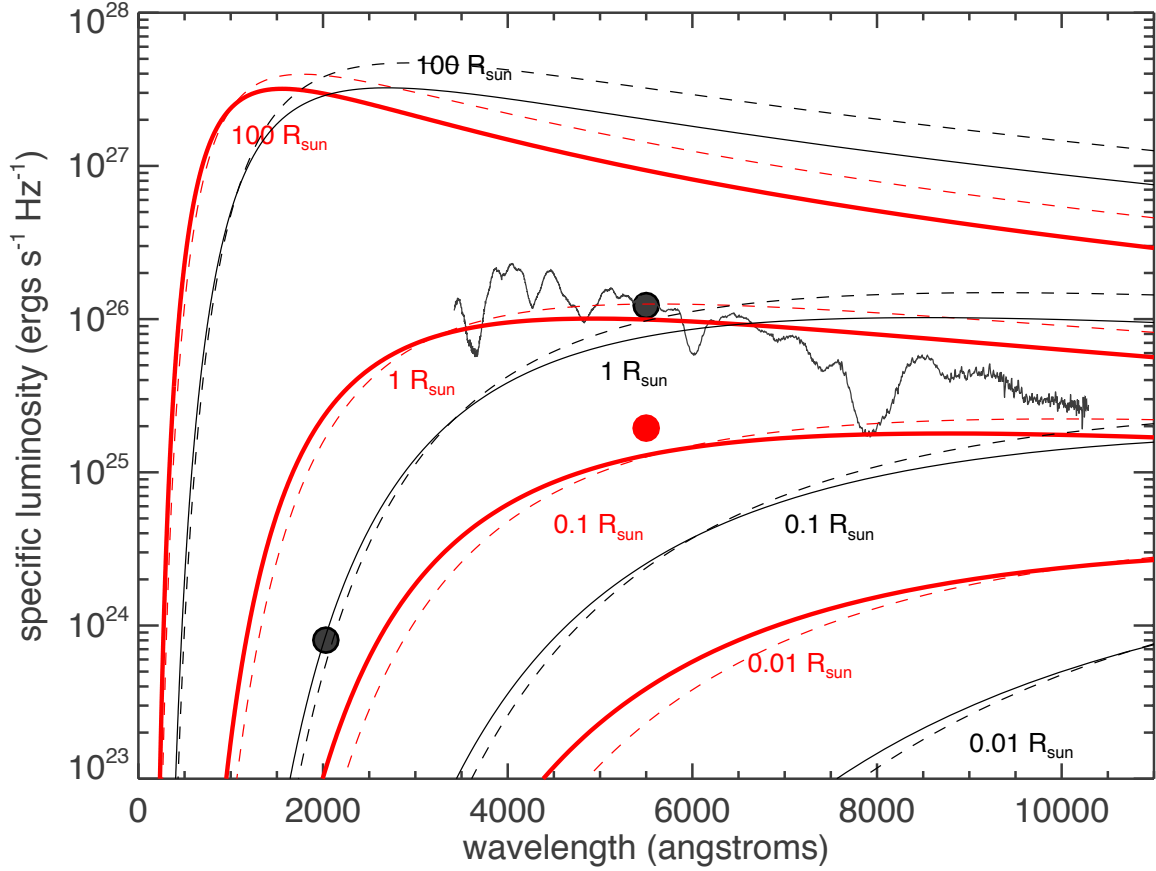
Figure 4: Models and early data limit the radius of the exploding star of SN 2011fe. The red lines show blackbody models for the day 0.5 spectrum assuming different values of the progenitor star radius R_0, where the solid lines and the dashed lines are derived from two separate analyses[19,27]. The observed *g*-band photometry point at this time (red circle) constrains the radius of the progenitor star (or the surrounding opaque circumstellar medium) to be $\leq 10^{10}$ cm ≈ 0.1 R$_\odot$. The black lines and circles show corresponding model predictions and observations at day 1.45. In all models, we have assumed an ejecta mass equal to the Chandrasekhar mass, an explosion energy of 10^{51} erg, and an opacity of 0.2 cm^2 g^{-1}, appropriate for electron scattering in a singly ionised $A/Z = 2$ medium. The early-time data indicate that the progenitor of SN 2011fe was a compact star, namely a white dwarf.

1   Supplementary Information

Low-Resolution Optical Spectroscopy: Our first spectra of SN 2011fe were obtained with the FRODOSpec instrument on the Liverpool Telescope (La Palma, Canary Islands, Spain). This dual-beam integral-field unit (IFU) spectrograph gives a resolving power of 2200. The supernova (SN) was observed on August 24, starting at 20.7 (UT dates are used throughout) with an exposure time of 1800 s. The wavelength coverage is 3900–5600 Å in the blue arm and 5900-9000 Å in the red arm. The raw spectra for each fiber of the IFU were extracted using a custom-built pipeline. This resulted in a sky-subtracted and wavelength-calibrated spectrum for each fiber. They were then combined together and a flux calibration was applied.

We also obtained low-resolution optical spectra of SN 2011fe with the Kast spectrograph[28] mounted on the 3 m Shane telescope at Lick Observatory beginning at 04:05 on 2011 August 25. It was taken with a $2''$ wide slit, and a 600/3410 grism on the blue side and a 300/7500 grating on the red side, resulting in full width at half-maximum (FWHM) resolutions of ~ 4 and 6 Å, respectively. The spectrum was aligned along the parallactic angle to reduce differential light losses[29]. All spectra were reduced using standard techniques. Routine CCD processing and spectrum extraction were completed with IRAF, and the data were extracted with an optimal algorithm[30]. We obtained the wavelength scale from low-order polynomial fits to calibration-lamp spectra. Small wavelength shifts were then applied to the data after cross-correlating a template sky to the night-sky lines that were extracted with the SN. We fit spectrophotometric standard-star spectra to the data in order to flux calibrate our spectra and to remove telluric lines[31, 32].

The results of these observations are plotted in Figure 2 of the main text.

High-Resolution Optical Spectroscopy: We observed SN 2011fe with the High Resolution Echelle Spectrometer (HIRES[33]) mounted on the 10 m Keck I telescope beginning at 5:51 on 2011 August 25 (only 1.6 day after our derived explosion date). The spectrum was reduced using standard techniques, and normalised by fitting the continuum in each echelle order with low-order polynomials. Wavelength calibration was performed relative to a series of emission-line lamps, and then corrected to the Solar System barycenter frame of reference. A cutout of the resulting normalised spectrum, centred on the rest-frame Na I $\lambda\lambda$5890, 5896 doublet, is shown in Figure 2 of the main text.

In this wavelength range, we identify only a single significant absorption feature. Fitting a Gaussian profile to this line, we measure a central wavelength of $\lambda = 5893.75 \pm 0.02$ Å and a FWHM of 0.184 ± 0.009 Å. The inferred line equivalent width is $W = 0.045 \pm 0.009$ Å.

If we associate this feature with Na I λ5890 (the stronger of the two components in the doublet), the observed wavelength is offset from the rest wavelength by $\Delta v = +194$ km s^{-1}. Similarly, the line is blueshifted from the systemic velocity of M101 ($v = 241 \pm 2$ km s^{-1})[34] by $\Delta v =$

$-47\,\mathrm{km\,s^{-1}}$. Given the high Galactic latitude ($b = 59.8°$), we consider it likely that the absorbing material originates in M101.

Independent of the origin of the absorbing material, the lack of strong Na I features indicates that the line of sight to SN 2011fe is affected by a negligible amount of extinction. Using common scaling relations[35], the observed equivalent width corresponds to an optical extinction of $A_V = 0.04\,\mathrm{mag}$.

Swift **UltraViolet/Optical Observations:** Immediately upon discovery we triggered target-of-opportunity observations of SN 2011fe with the *Swift* satellite[36]. Observations with the UltraViolet-Optical Telescope (UVOT[37]) began at 22:08 on 24 August 2011. We retrieved the level 2 UVOT data for SN 2011fe from the *Swift* data archive. To increase the signal-to-noise ratio, we stacked the images for each individual filter on a daily basis. To remove host-galaxy contamination underlying the SN location, we subtracted pre-outburst images of M101 obtained by the UVOT. We caution that, due to the nonlinearity of the coincidence-loss correction, such a technique can lead to modest systematic uncertainties in the SN flux, particularly at high count rates[38]. The photometric calibration was performed following standard recipes[39], and the reported magnitudes are on the AB system[40]. The resulting photometry is presented in Supplementary Table 1.

SYNAPPS Spectral Fits: We analysed the spectrum of SN 2011fe using the automated SN spectrum interpretation code SYNAPPS[10]. SYNAPPS uses a parallelised pattern search algorithm to compare highly parametrised synthetic spectra to observed ones to find a good fit. Results from SYNAPPS are useful for (a) identifying or rejecting the presence of ion signatures and (b) estimating characteristic ejecta velocities. Typical premaximum SN Ia ions are confirmed: O I, Mg II, Si II, S II, Ca II, and Fe II (Supplementary Figure 1). Fe III was not needed in the fit. In addition, the fit confirms the presence of C II $\lambda\lambda 6580, 7234$, though the detailed fit is not perfect, probably due to parametrisation bias. Both high-velocity (HV) Si II and Ca II are confirmed by SYNAPPS (extending above 21,000 km/s). Surprisingly, SYNAPPS finds HV O I (in excess of 20,000 km/s) for the absorption centered at 7400 Å. This is the first identification of variable high-velocity oxygen in the ejecta of a SN Ia in the literature to date. Furthermore we note that the change in velocity of the Mg II and Fe II features are ~4% and that of Si II is ~8% over the first 24 hr.

Parabolic Shape of the ^{56}Ni Powered Light Curve at Early Times: The $L \propto t^2$ behaviour found for the early-time light curve of SN 2011fe is consistent with a simple fireball model in which the effective temperature remains fixed while the radius increases with time as $r = v_p t$. In reality, one expects the effective temperature to change with time, while the photospheric velocity v_p will decrease as the remnant expands and the density drops. However, the same t^2 law can be derived by a more rigorous analytic argument that includes the effects of radiative diffusion, ^{56}Ni energy deposition, and expansion losses[41]. We describe here a simple one-spatial-zone model for the whole remnant which shows that the observed rise, $L \propto t^2$ at early times, is consistent with a ^{56}Ni powered SN, with no contribution to the luminosity from the explosion shock wave or from

MJD	Telescope/Instrument	Filter	Exp. Time (s)	Magnitude
55795.199	P48	*g*	120.0	> 21.5
55797.166	P48	*g*	60.0	17.349 ± 0.011
55797.209	P48	*g*	60.0	17.155 ± 0.011
55797.923	*Swift*/UVOT	*uvw*1	314.49	18.90 ± 0.21
55797.925	*Swift*/UVOT	*u*	157.04	16.68 ± 0.05
55797.926	*Swift*/UVOT	*b*	157.02	15.42 ± 0.09
55797.927	*Swift*/UVOT	*uvw*2	629.48	20.96 ± 0.39
55797.930	*Swift*/UVOT	*v*	157.02	15.12 ± 0.09
55797.931	*Swift*/UVOT	*uvm*2	3264.03	> 21.0
55798.156	P48	*g*	60.0	14.886 ± 0.010
55798.199	P48	*g*	60.0	14.839 ± 0.009
55799.001	*Swift*/UVOT	*uvw*1	618.60	17.35 ± 0.08
55799.002	*Swift*/UVOT	*u*	206.69	15.11 ± 0.03
55799.003	*Swift*/UVOT	*b*	206.63	13.86 ± 0.06
55799.003	*Swift*/UVOT	*uvw*2	1037.48	19.02 ± 0.26
55799.006	*Swift*/UVOT	*v*	276.45	13.62 ± 0.06
55799.006	*Swift*/UVOT	*uvm*2	1387.15	20.04 ± 0.29
55799.142	P48	*g*	30.0	13.787 ± 0.011
55799.164	P48	*g*	30.0	13.751 ± 0.013
55799.181	P48	*g*	30.0	13.713 ± 0.011
55799.202	P48	*g*	30.0	13.726 ± 0.013
55799.221	P48	*g*	30.0	13.701 ± 0.013
55799.239	P48	*g*	30.0	13.689 ± 0.012
55800.203	P48	*g*	30.0	12.964 ± 0.013
55800.221	P48	*g*	30.0	12.959 ± 0.012

Table 1: UV/Optical Observations of SN 2011fe. P48 observations have been calibrated with respect to Sloan Digital Sky Survey *g*-band images of the field, and are on the PTF photometric system. *Swift*/UVOT images have been calibrated using standard recipes[39] and are reported on the AB system[40].
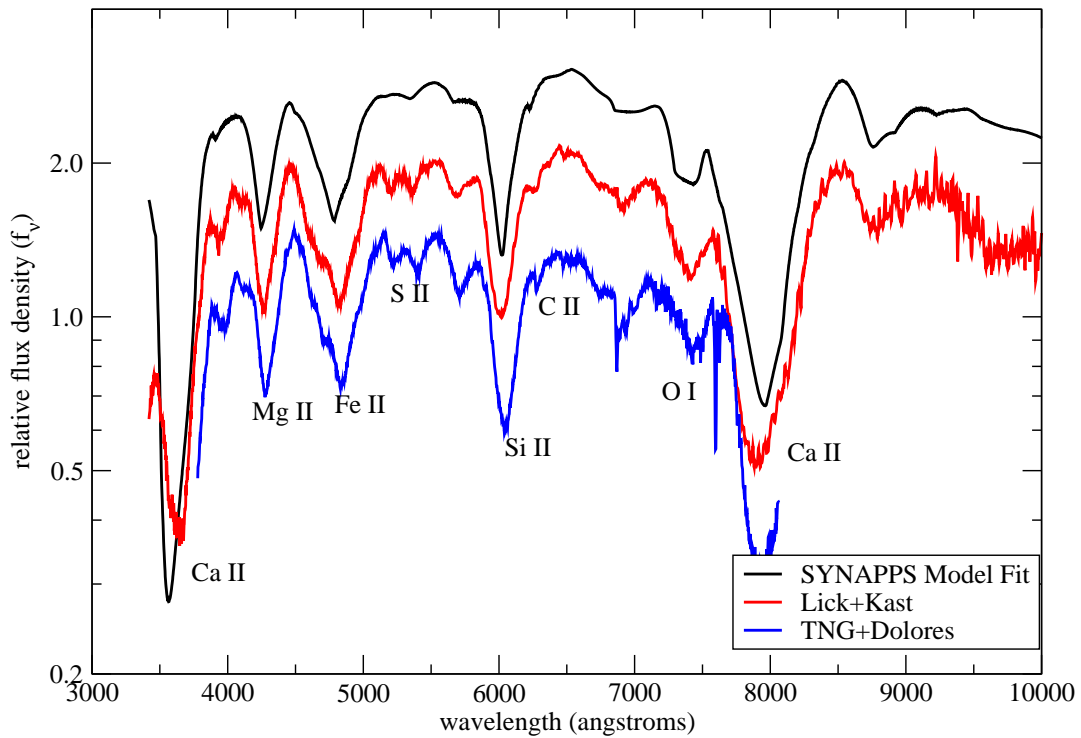
Figure 5: A SYNAPPS fit to the Lick/Kast spectrum and the TNG/Dolores spectrum taken 16 hrs later. The agreement is excellent and we have confidently identified several intermediate-mass elements including high-velocity Ca II, Si II, and O I, the last of which forms the feature centered at 7400 Å.

interaction with circumstellar material or a companion star.

For the expanding remnant, the evolution of the internal energy, E_{int}, is given by the first law of thermodynamics,

$$\frac{\partial E_{int}}{\partial t} = -P\frac{\partial V}{\partial t} + L_{Ni}(t) - L_e(t), \tag{1}$$

where L_{Ni} is the energy deposited per second from ^{56}Ni decay and L_e is the radiated luminosity. We assume that the ^{56}Ni energy is thermalised throughout the remnant, and that radiation pressure dominates, $P = E_{int}/3V$. Assuming homologous expansion, the volume increases as $V \propto t^3$ and equation 1 becomes

$$\frac{1}{t}\frac{\partial}{\partial t}[E_{int}t] = L_{Ni}(t) - L_e(t). \tag{2}$$

The radiated luminosity, L_e, is approximated from the diffusion equation

$$\frac{L_e}{4\pi R^2} = \frac{c}{3\kappa\rho}\frac{\partial E_{int}/V}{\partial r} \approx \frac{c}{3\kappa\rho}\frac{E_{int}/V}{R}. \tag{3}$$

In homologous expansion, $R = v_f t$, and the radiated luminosity can be rewritten

$$L_e = \frac{E_{int}t}{t_d^2}, \quad \text{where} \quad t_d = \left[\frac{3}{4\pi}\frac{M_{ej}\kappa}{v_f c}\right]^{1/2}. \tag{4}$$

Here, we defined the effective diffusion time t_d, and $v_f = [E_{sn}/2M_{ej}]^{1/2}$ is the final characteristic ejecta velocity. For the case where the elapsed time is much less than the ^{56}Ni decay time of $\tau_{Ni} = 8.8$ day, the energy deposition from ^{56}Ni decay can be considered constant with time ($L_{Ni} = E_{Ni}/\tau_{Ni}$) and the solution of equation 4 is

$$L_e(t) \approx \frac{E_{Ni}}{\tau_{Ni}}[1 - e^{-t^2/2t_d^2}] \qquad t \ll \tau_{Ni}, \tag{5}$$

where we have assumed that the initial internal energy of the ejecta (from the explosion shock) is negligible compared to the heating from ^{56}Ni decay. For typical parameters, the effective diffusion time is ~ 20 day, so taking the limit $t \ll t_d$ gives

$$L_e(t) \approx \frac{E_{Ni}}{\tau_{Ni}}\frac{t^2}{2t_d^2} \qquad t \ll t_d, t \ll \tau_{Ni}. \tag{6}$$

The validity of the argument can be questioned at these very early times, as the analysis does not properly capture the early transient phase in which a diffusion wave moves from the inner ^{56}Ni core to the surface. However, the excellent fit of the observed light curve to a t^2 law suggests that the simple model is not unreasonable. From the day 0.45 observation of SN 2011fe (luminosity $L \approx 10^{40}\,\text{erg s}^{-1}$) and equation 6, we find a total ^{56}Ni mass of 0.45 $M_\odot$, comparable to the value inferred for a (slightly underluminous) normal SN Ia. This suggests that the early-time luminosity of SN 2011fe is consistent with ^{56}Ni powering only, with little or no contribution from shocks.

5

Contribution to the Early Luminosity from Shock Heating: At early times (~ 1 day), the diffusion of radiation from the ejecta shock-heated in the explosion may contribute to the emergent luminosity (in addition to the luminosity generated by ^{56}Ni heating). Observations of this shock luminosity can be used to constrain the radius of the progenitor star. Relevant models have been considered by many authors[18,42–47], all of whom take a similar analytical approach to calculating the evolution of a radiation dominated, homologously expanding, constant opacity, spherically symmetric supernova remnant. The models differ in their assumptions of the initial ejecta density and pressure profiles and in the treatment of radiative diffusion. However, the final predictions of the early-time light curve tend to be quite similar.

Recent work has shown[47], for the case of early cooling luminosity after shock breakout in a SN Ia, the luminosity and effective temperature follow:

$$
\begin{aligned}
L(t) &= 1.2 \times R_{10} 10^{40} E_{51}^{0.85} M_c^{-0.69} \kappa_{0.2}^{-0.85} f_p^{-0.16} t_d^{-0.31} \text{ erg s}^{-1}, \\
T(t) &= 4015\, R_{10}^{1/4} E_{51}^{0.016} M_c^{0.03} \kappa_{0.2}^{0.27} f_p^{-0.022} t_d^{-0.47} \text{ K},
\end{aligned}
\tag{7}
$$

where E_{51} is the explosion energy $E/10^{51}$ erg, R_{10} is the progenitor radius $R/10^{10}$ cm, M_c is the total ejecta mass in units of the Chandrasekhar mass, $\kappa_{0.2}$ is the opacity $\kappa/0.2$ cm^2 g^{-1}, f_p is a dimensionless form factor, and t_d is the time since explosion in days. These results are similar to those found by earlier work[18] for ejecta in spherical expansion.

For the case of SN ejecta impacting a companion star in Roche-lobe overflow, self-similar diffusion arguments have shown that the post interaction luminosity is described by[44]:

$$
\begin{aligned}
L(t) &= 1.0 \times 10^{40} a_{10}\, E_{51}^{0.875} M_c^{-0.375} \kappa_{0.2}^{-0.75} t_d^{-0.5} \text{ erg s}^{-1}, \\
T(t) &= 4446\, a_{10}^{1/4} E_{51}^{0.0} M_c^{0.0} \kappa_{0.2}^{0.97} t_d^{-0.51} \text{ K},
\end{aligned}
\tag{8}
$$

where a_{10} is the separation distance between the WD and its companion star in units of 10^{10} cm. The isotropic equivalent luminosity here applies to a viewing angle aligned with the symmetry axis, and will be lower for off-axis viewing angles. Despite the somewhat different context and approach, the formulae are very similar to the previously discussed colling of the shock heated SN[47], both in the scalings and the overall normalization. In particular, the luminosity depends linearly on R or a, while the effective temperature is proportional to $R^{1/4}$ or $a^{1/4}$.

We used equations 7 and 8 to construct model spectra for progenitors of different radii. We assumed values typical of SN Ia models, namely $E_{51} = 1, M_c = 1, \kappa_{0.2} = 1, f_p = 1$. The emission spectrum was taken to be a blackbody with temperature T and luminosity L. The day 0.45 g-band observation of SN 2011fe indicates $L \sim 10^{40}$ erg s^{-1}, which constrains the progenitor radius to $R \le 10^{10}$ cm.

Because the impact with a companion star only shocks a portion of the SN ejecta (that within a conical region with opening angle $\sim 40°$), the shock luminosity from the interaction

6

is anisotropic, and will be most prominent for viewing angles nearly aligned with the symmetry axis. Such an orientation occurs $\sim 10\%$ of the time. Numerical multi-dimensional radiation transport calculations of the dependence of the luminosity on viewing angle[44] show that the luminosity observed $90°$ ($180°$) from the symmetry axis is about a factor 10 (100) lower than that viewed on-axis. For a red-giant companion ($a \approx 10^{13}$ cm), the predicted shock luminosity is $\geq 10^{41}$ erg s^{-1} for all viewing angles, ruling out this progenitor system. A $1\,M_\odot$ main-sequence companion ($a \approx 10^{11}$ cm) has $L \approx 10^{41}$ erg s^{-1} when viewed on-axis, and thus would be consistent with the data if the observer were oriented $\geq 90°$ from the symmetry axis.

1. Riess, A. G., *et al.*, Observational Evidence from Supernovae for an Accelerating Universe and a Cosmological Constant. *Astron. J.* **116**, 1009–1038, September (1998).

2. Perlmutter, S., *et al.*, Measurements of Omega and Lambda from 42 High-Redshift Supernovae. *Astrophys. J.* **517**, 565–586, June (1999).

3. Sullivan, M., *et al.*, SNLS3: Constraints on Dark Energy Combining the Supernova Legacy Survey Three-year Data with Other Probes. *Astrophys. J.* **737**, 102–121, August (2011).

4. Howell, D. A. Type Ia supernovae as stellar endpoints and cosmological tools. *Nature Communications* **2**, June (2011).

5. Kasen, D., Röpke, F. K. and Woosley, S. E., The diversity of type Ia supernovae from broken symmetries. *Nature* **460**, 869–872, August (2009).

6. Yoon, S.-C., Podsiadlowski, P., and Rosswog, S. Remnant evolution after a carbon-oxygen white dwarf merger. *Mon. Not. R. Astron. Soc.* **380**, 933–948, September (2007).

7. Shappee, B. J. and Stanek, K. Z. A New Cepheid Distance to the Giant Spiral M101 Based on Image Subtraction of Hubble Space Telescope/Advanced Camera for Surveys Observations. *Astrophys. J.* **733**, 124–149, June (2011).

8. Li, W. *et al.*, *Nature*, this issue, (2011).

9. Nugent, P. E., Sullivan, M., Bersier, D., Howell, D. A., Thomas, R., and James, P. Young Type Ia Supernova PTF11kly in M101. *The Astronomer's Telegram* **3581**, 1, August (2011).

10. Thomas, R. C., Nugent, P. E., and Meza, J. C. SYNAPPS: Data-Driven Analysis for Supernova Spectroscopy. *Pub. Astron. Soc. Pac.* **123**, 237–248, February (2011).

11. Filippenko, A. V. Optical Spectra of Supernovae. *Ann. Rev. Astron. & Astrophys.* **35**, 309–355 (1997).

12. Branch, D., Lacy, C. H., McCall, M. L., Sutherland, P. G., Uomoto, A., Wheeler, J. C., and Wills, B. J. The Type I supernova 1981b in NGC 4536 - The first 100 days. *Astrophys. J.* **270**, 123–125, July (1983).

13. Leibundgut, B., *et al.*, Premaximum observations of the type IA SN 1990N. *Astrophys. J. Let.* **371**, L23–L26, April (1991).

14. Nugent, P., Phillips, M., Baron, E., Branch, D., and Hauschildt, P. Evidence for a Spectroscopic Sequence among Type 1a Supernovae. *Astrophys. J. Let.* **455**, L147–L151, December (1995).

15. Kirshner, R. P., *et al.*, SN 1992A: Ultraviolet and Optical Studies Based on HST, IUE, and CTIO Observations. *Astrophys. J.* **415**, 589–615, October (1993).

16. Patat, F., *et al.*, The type IA supernova 1994D in NGC 4526: the early phases. *Mon. Not. R. Astron. Soc.* **278**, 111–124, January (1996).

17. Hatano, K., Branch, D., Fisher, A., Baron, E., and Filippenko, A. V. On the High-Velocity Ejecta of the Type IA Supernova SN 1994D. *Astrophys. J.* **525**, 881–885, November (1999).

18. Piro, A. L., Chang, P., and Weinberg, N. N. Shock Breakout from Type Ia Supernova. *Astrophys. J.* **708**, 598–604, January (2010).

19. Kasen, D. Seeing the Collision of a Supernova with Its Companion Star. *Astrophys. J.* **708**, 1025–1031, January (2010).

20. Fryer, C. L., *et al.*, Spectra of Type Ia Supernovae from Double Degenerate Mergers. *Astrophys. J.* **725**, 296–308, December (2010).

21. Shen, K. J., Bildsten, L., Kasen, D., and Quataert, E. The Long-Term Evolution of Double White Dwarf Mergers. arXiv e-prints (astro-ph/1108.4036), August (2011).

22. Rau, A., *et al.*, Exploring the Optical Transient Sky with the Palomar Transient Factory. *Pub. Astron. Soc. Pac.* **121**, 1334–1351, December (2009).

23. Law, N. M., *et al.*, The Palomar Transient Factory: System Overview, Performance, and First Results. *Pub. Astron. Soc. Pac.* **121**, 1395–1408, December (2009).

24. Gal-Yam, A., *et al*, Real-time Detection and Rapid Multiwavelength Follow-up Observations of a Highly Subluminous Type II-P Supernova from the Palomar Transient Factory Survey. *Astrophys. J.* **736**, 159–166, August (2011).

25. Bloom, J. S., *et al.*, Automating Discovery and Classification of Transients and Variable Stars in the Synoptic Survey Era. arXiv e-prints (astro-ph/1106.5491), June (2011).

26. de Vaucouleurs, G., de Vaucouleurs, A., Corwin, Jr., H. G., Buta, R. J., Paturel, G., and Fouque, P. *Third Reference Catalogue of Bright Galaxies*. (1991).

27. Rabinak, I., Livne, E., and Waxman, E. Early emission from type Ia supernovae. arXiv e-prints (astro-ph/1108.5548), August (2011).

28. Miller, J. S. and Stone, R. P. S. Lick Obs. Tech. Rep. 66. Lick Obs., Santa Cruz (1993).

29. Filippenko, A. V. The importance of atmospheric differential refraction in spectrophotometry. *Pub. Astron. Soc. Pac.* **94**, 715–721, August (1982).

30. Horne, K. An optimal extraction algorithm for ccd spectroscopy. *Pub. Astron. Soc. Pac.* **98**, 609, Jun (1986).

31. Wade, R. A. and Horne, K. The radial velocity curve and peculiar tio distribution of the red secondary star in z chamaeleontis. *Astrophys. J.* **324**, 411, Jan (1988).

32. Matheson, T., Filippenko, A. V., Ho, L. C., Barth, A. J., and Leonard, D. C. Detailed analysis of early to late-time spectra of supernova 1993j. *Astron. J.* **120**, 1499, Sep (2000).

33. Vogt, S. S., Allen, S. L., Bigelow, B. C., Bresee, L., Brown, B., Cantrall, T., Conrad, A., Couture, M., Delaney, C., Epps, H. W., Hilyard, D., Hilyard, D. F., Horn, E., Jern, N., Kanto, D., Keane, M. J., Kibrick, R. I., Lewis, J. W., Osborne, J., Pardeilhan, G. H., Pfister, T., Ricketts, T., Robinson, L. B., Stover, R. J., Tucker, D., Ward, J., and Wei, M. Z. HIRES: the high-resolution echelle spectrometer on the Keck 10-m Telescope. In Society of Photo-Optical Instrumentation Engineers (SPIE) Conference Series, D. L. Crawford & E. R. Craine, editor, volume 2198 of *Society of Photo-Optical Instrumentation Engineers (SPIE) Conference Series*, 362, June (1994).

34. de Vaucouleurs, G., de Vaucouleurs, A., Corwin, Jr., H. G., Buta, R. J., Paturel, G., and Fouqué, P. *Third Reference Catalogue of Bright Galaxies. Volume I: Explanations and references. Volume II: Data for galaxies between 0^h and 12^h. Volume III: Data for galaxies between 12^h and 24^h.* (1991).

35. Munari, U. and Zwitter, T. Equivalent width of NA I and K I lines and reddening. *Astron. & Astrophys.* **318**, 269–274, February (1997).

36. Gehrels, N., Chincarini, G., Giommi, P., Mason, K. O., Nousek, J. A., Wells, A. A., White, N. E., Barthelmy, S. D., Burrows, D. N., Cominsky, L. R., Hurley, K. C., Marshall, F. E., Mészáros, P., Roming, P. W. A., Angelini, L., Barbier, L. M., Belloni, T., Campana, S., Caraveo, P. A., Chester, M. M., Citterio, O., Cline, T. L., Cropper, M. S., Cummings, J. R., Dean, A. J., Feigelson, E. D., Fenimore, E. E., Frail, D. A., Fruchter, A. S., Garmire, G. P., Gendreau, K., Ghisellini, G., Greiner, J., Hill, J. E., Hunsberger, S. D., Krimm, H. A., Kulkarni, S. R., Kumar, P., Lebrun, F., Lloyd-Ronning, N. M., Markwardt, C. B., Mattson, B. J., Mushotzky, R. F., Norris, J. P., Osborne, J., Paczynski, B., Palmer, D. M., Park, H.-S., Parsons, A. M., Paul, J., Rees, M. J., Reynolds, C. S., Rhoads, J. E., Sasseen, T. P., Schaefer, B. E., Short, A. T., Smale, A. P., Smith, I. A.,. The Swift Gamma-Ray Burst Mission. *Astrophys. J.* **611**, 1005–1020, August (2004).

37. Roming, P. W. A., Kennedy, T. E., Mason, K. O., Nousek, J. A., Ahr, L., Bingham, R. E., Broos, P. S., Carter, M. J., Hancock, B. K., Huckle, H. E., Hunsberger, S. D., Kawakami, H., Killough, R., Koch, T. S., McLelland, M. K., Smith, K., Smith, P. J., Soto, J. C., Boyd, P. T., Breeveld, A. A., Holland, S. T., Ivanushkina, M., Pryzby, M. S., Still, M. D., and Stock, J. The Swift Ultra-Violet/Optical Telescope. Space Sci. Rev. **120**, 95–142, October (2005).

38. Brown, P. J., Holland, S. T., Immler, S., Milne, P., Roming, P. W. A., Gehrels, N., Nousek, J., Panagia, N., Still, M., and Vanden Berk, D. Ultraviolet Light Curves of Supernovae with the Swift Ultraviolet/Optical Telescope. *Astron. J.* **137**, 4517–4525, May (2009).

39. Poole, T. S., Breeveld, A. A., Page, M. J., Landsman, W., Holland, S. T., Roming, P., Kuin, N. P. M., Brown, P. J., Gronwall, C., Hunsberger, S., Koch, S., Mason, K. O., Schady, P., vanden Berk, D., Blustin, A. J., Boyd, P., Broos, P., Carter, M., Chester, M. M., Cucchiara, A., Hancock, B., Huckle, H., Immler, S., Ivanushkina, M., Kennedy, T., Marshall, F., Morgan, A., Pandey, S. B., de Pasquale, M., Smith, P. J., and Still, M. Photometric calibration of the Swift ultraviolet/optical telescope. *Mon. Not. R. Astron. Soc.* **383**, 627–645, January (2008).

10

40. Oke, J. B. and Gunn, J. E. Secondary standard stars for absolute spectrophotometry. *Astrophys. J.* **266**, 713, Mar (1983).

41. Arnett, W. D. Type I supernovae. I - Analytic solutions for the early part of the light curve. *Astrophys. J.* **253**, 785–797, February (1982).

42. Chevalier, R. A. Early expansion and luminosity evolution of supernovae. *Astrophys. J.* **394**, 599–602, August (1992).

43. Chevalier, R. A. and Fransson, C. Shock Breakout Emission from a Type Ib/c Supernova: XRT 080109/SN 2008D. *Astrophys. J. Let.* **683**, L135–L138, August (2008).

44. Kasen, D. Seeing the Collision of a Supernova with Its Companion Star. *Astrophys. J.* **708**, 1025–1031, January (2010).

45. Nakar, E. and Sari, R. Relativistic shock breakouts - a variety of gamma-ray flares: from low luminosity gamma-ray bursts to type Ia supernovae. *ArXiv e-prints*, June (2011).

46. Rabinak, I. and Waxman, E. The Early UV/Optical Emission from Core-collapse Supernovae. *Astrophys. J.* **728**, 63–+, February (2011).

47. Rabinak, I., Livne, E., and Waxman, E. Early emission from type Ia supernovae. *ArXiv e-prints*, August (2011).